DOI: 10.1002/cmdc.201100284

Derivatives of Benzimidazol-2-ylquinoline and Benzimidazol-2-ylisoquinoline as Selective A_1 Adenosine Receptor Antagonists with Stimulant Activity on Human Colon Motility

Barbara Cosimelli,*[a] Sabrina Taliani,*[b] Giovanni Greco,[a] Ettore Novellino,[a] Annalisa Sala,[a] Elda Severi,[a] Federico Da Settimo,[b] Concettina La Motta,[b] Isabella Pugliesi,[b] Luca Antonioli,[c] Matteo Fornai,[c] Rocchina Colucci,[c] Corrado Blandizzi,[c] Simona Daniele,[d] Maria Letizia Trincavelli,[e] and Claudia Martini[e]

A number of quinolines and isoquinolines connected in various ways to a substituted benzimidazol-2-yl system were synthesized and evaluated as novel antagonists of adenosine receptors (ARs) by competition experiments using human A_1, A_{2A}, and A_3 ARs. The new compounds were designed based on derivatives of 2-(benzimidazol-2-yl)quinoxaline, previously reported as potent and selective antagonists of A_1 and A_3 ARs. Among these, 3-[4-(ethylthio)-1*H*-benzimidazol-2-yl]isoquinoline **4b** exhibited the best combination of potency toward the A_1 AR ($K_i = 1.4$ nM) and selectivity against the A_{2A} ($K_i > 10$ μM), A_{2B} ($K_i > 10$ μM), and A_3 ARs ($K_i > 1$ μM). Functional experiments in circular smooth muscle preparations of isolated human colon showed that **4b** behaves as a potent and selective antagonist of the A_1 AR in the neuromuscular compartment of this intestinal region. Biological and pharmacological data suggest that **4b** is a suitable starting point for the development of novel agents endowed with stimulant properties on colonic activity.

Introduction

Adenosine is an endogenous signaling nucleoside that is released from several cells and plays a key role in a variety of physiological processes.[1–4] Once in the extracellular space, adenosine can affect cell functioning by triggering specific G-protein-coupled receptors which modulate a number of effector systems, including adenylate cyclase, potassium and calcium channels, phospholipase C or D, and guanylate cyclase.[5] Four adenosine receptor (AR) subtypes, classified as A_1, A_{2A}, A_{2B}, and A_3, have been identified as mediators of these effects.[3] Each receptor subtype has been indicated as a target for the development of agonist- and antagonist-based therapies against a wide range of pathologies, including central nervous system (CNS) disorders, cardiac arrhythmia, ischemic injuries, asthma, renal failure, and inflammatory diseases.[1,6,7] The A_1 AR has been extensively investigated due to its important biological role in various tissues such as CNS, heart, kidneys, liver, and bladder.[8] Selective A_1 AR antagonists may be useful in cognition enhancement for the treatment of various forms of dementia, including Alzheimer's disease.[9–11] A_1 AR antagonists are also under development as potassium-sparing diuretics with kidney-protective properties and for treatment of acute renal failure.[8,12,13]

Fornai et al.[14] demonstrated that adenosine contributes significantly to the enteric regulatory network that is dependent on modulation of human colonic motility. In particular, it was observed that the A_1 AR is actively involved in tonic inhibitory actions exerted by endogenous adenosine on the excitatory cholinergic motility of the colon. Furthermore, in the presence of inflammatory intestinal conditions, the modulation of ARs or enzymes driving adenosine metabolism can favorably affect the outcome of inflammation as well as the related digestive motor alterations.[15–21] Studies on the effects of novel A_1 AR antagonists on the contractile function of human colon could pave the way to the discovery of new options for the therapeutic management of digestive disorders characterized by decreased gastrointestinal propulsion, such as idiopathic chronic constipation, irritable bowel syndrome with predominance of constipation, and post-operative paralytic ileus.[19,22] Postoperative ileus (POI) is a common adverse event associated with ab-

[a] *Prof. B. Cosimelli, Prof. G. Greco, Prof. E. Novellino, Dr. A. Sala, Dr. E. Severi*
Dipartimento di Chimica Farmaceutica e Tossicologica
Università di Napoli "Federico II", Via D. Montesano 49, 80131 Napoli (Italy)
E-mail: barbara.cosimelli@unina.it

[b] *Dr. S. Taliani, Prof. F. Da Settimo, Dr. C. La Motta, Dr. I. Pugliesi*
Dipartimento di Scienze Farmaceutiche
Università di Pisa, Via Bonanno 6, 56126 Pisa (Italy)
E-mail: taliani@farm.unipi.it

[c] *Dr. L. Antonioli, Dr. M. Fornai, Dr. R. Colucci, Prof. C. Blandizzi*
Centro Interdipartimentale di Ricerche di Farmacologia Clinica e Terapia Sperimentale, Università di Pisa, Via Roma 55, 56126 Pisa (Italy)

[d] *Dr. S. Daniele*
Department of Drug Discovery and Development
Istituto Italiano di Tecnologia, via Morego, 30, 16163 Genova (Italy)

[e] *Dr. M. L. Trincavelli, Prof. C. Martini*
Dipartimento di Psichiatria, Neurobiologia, Farmacologia e Biotecnologie
Università di Pisa, Via Bonanno 6, 56126 Pisa (Italy)

Supporting information for this article is available on the WWW under http://dx.doi.org/10.1002/cmdc.201100284.

dominal surgical procedures and is believed to occur as a result of inhibitory neural reflexes and local inflammatory processes.[23] Prolonged POI can lead to patient discomfort, decreased mobility, delayed enteral feeding, and, ultimately, prolonged hospitalizations and increased social costs. At present, limited pharmacological strategies are available to effectively and successfully decrease the duration of POI.[23] Blockade of the A_1 AR by highly potent and selective antagonists may provide a novel option to favorably affect POI duration.

We recently described the synthesis and biological evaluation of 2-(1*H*-benzimidazol-2-yl)quinoxalines **1** as A_1 and A_3 AR antagonists, which were designed on the basis of database searches and lead optimization approaches (Figure 1).[24] Specifically, the Cambridge Structural Database (CSD)[25] (version 5.25) was scanned using a pharmacophore substructure with a 3D disposition defined by torsion angles. One of the hits resulting from this search was 2,3-bis(1*H*-benzimidazol-2-yl)quinoxaline (CSD reference code *bzquxl*).[24] This structure was translated synthetically into analogues devoid of one of the two benzimidazole systems, based on the assumption that the less bulky (1*H*-benzimidazol-2-yl)quinoxalines **1** would be more suitable for binding to the target receptors (Figure 1). Among the tested compounds from series **1** (see Figure 4 below), the compounds exhibiting the highest affinity for A_1 and A_3 ARs were 2-[4-(ethylthio)-1*H*-benzimidazol-2-yl]quinoxaline **1b** (K_i values at the A_1, A_{2A}, and A_3 ARs of 0.5, 3440, and 955 nM, respectively) and 2-[4-methyl-1*H*-benzimidazol-2-yl]quinoxaline **1d** (K_i values at the A_1, A_{2A}, and A_3 ARs of 8000, 833, and 26 nM, respectively) (Table 1).[24]

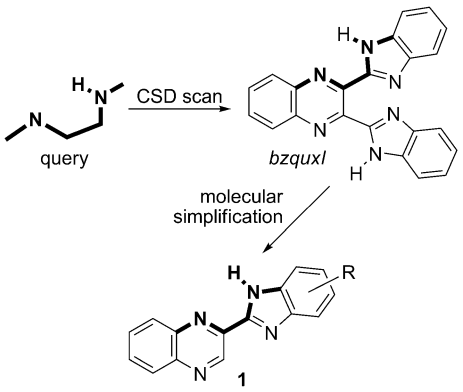

Figure 1. Design strategy leading to the discovery of (1*H*-benzimidazol-2-yl)quinoxalines **1** as A_1 and A_3 AR antagonists.

Prompted by the ease of synthesis for compounds in series **1** (obtained by condensing the quinoxaline-2-carboxylic acid with the appropriate *o*-phenylenediamine), we turned our attention to analogues of **1** that could be similarly prepared by a one-step procedure. A majority of the new scaffolds **2**–**5** were made by connecting a quinoline or isoquinoline nucleus to a substituted 1*H*-benzimidazol-2-yl system (Figure 2). All of the designed structures share a common pharmacophore composed of two nitrogen atoms with hydrogen bonding properties connected by two or three sp^2 carbons. The substituents attached to the benzimidazole ring were chosen from those that exhibited the best results in our previous work[24] (CH_3, Cl, SCH_3, SC_2H_5, or a fused benzene-cyclohexane ring to mimic disubstitution).

Table 1. Affinities for human A_1, A_{2A}, and A_3 ARs of the newly investigated compounds **2**–**5**, along with selected previously reported compounds **1**.

Compd	R^1	R^2	R^3	K_i [nM][a] hA_1[b]	hA_{2A}[c]	hA_3[d]
1a[e]	H	H	H	50.0 ± 15.0	561.0 ± 17.0	763.0 ± 13.0
1b[e]	SC_2H_5	H	H	0.50 ± 0.01	3440.0 ± 297.0	955.0 ± 88.0
1c[e]	SCH_3	H	H	2.10 ± 0.30	3000.0 ± 200.0	278.0 ± 44.0
1d[e]	CH_3	H	H	8000.0 ± 567.0	833.0 ± 67.0	26.0 ± 9.0
1i[e]	H	CH_3	CH_3	> 10000	> 10000	370.0 ± 35.0
2a	H	H	H	13.0 ± 0.1	1028.0 ± 95.1	225.2 ± 13.0
2b	SCH_3	H	H	> 10000	> 10000	280.2 ± 15.0
2c	CH_3	H	H	> 10000	> 10000	685.1 ± 111.0
2d	Cl	H	H	> 10000	> 10000	178.1 ± 17.0
2e	H	CH_3	H	20.7 ± 1.5	1342.3 ± 65.1	772.9 ± 4.0
2f	H	Cl	H	9.1 ± 0.4	> 10000	413.3 ± 16.0
2g	CH_3	H	Cl	2.9 ± 0.5	> 10000	828.0 ± 15.0
2h	Cl	H	Cl	> 10000	> 10000	174.0 ± 17.2
2i	H	CH_3	CH_3	14.5 ± 1.1	> 10000	> 1000
2j	H	Cl	Cl	> 10000	> 10000	> 1000
2k	CH_3	H	CH_3	> 10000	> 10000	660.2 ± 65.1
2l	–	–	–	> 10000	776.0 ± 14.2	653.0 ± 41.1
2m	–	–	–	> 10000	934.4 ± 56.2	> 1000
2n	–	–	–	> 10000	1330.3 ± 129.1	144.1 ± 14.0
2o	–	–	–	> 10000	> 10000	94.1 ± 5.0
2p	–	–	–	> 10000	> 10000	> 1000
3a	H	H	H	41.0 ± 3.1	1330.4 ± 105.2	415.0 ± 40.1
3b	SC_2H_5	H	H	273.2 ± 33.1	158.0 ± 7.2	> 1000
3c	CH_3	H	H	4.2 ± 0.3	277.1 ± 18.0	> 1000
3d	Cl	H	H	4.4 ± 0.1	195.2 ± 15.0	445.1 ± 28.2
3e	H	CH_3	H	162.0 ± 12.0	152.0 ± 11.3	200.3 ± 14.1
3f	H	Cl	H	19.3 ± 1.6	146.0 ± 11.1	307.2 ± 24.0
3g	CH_3	H	Cl	> 10000	1520.1 ± 150.2	272.0 ± 16.1
3h	Cl	H	Cl	> 10000	739.3 ± 33.1	509.4 ± 41.2
3i	H	CH_3	CH_3	> 10000	347.3 ± 31.1	19.2 ± 2.0
3j	H	Cl	Cl	> 10000	2744.1 ± 260.0	143.2 ± 5.3
3k	CH_3	H	CH_3	> 10000	> 10000	533.8 ± 52.5
3l	–	–	–	441.4 ± 44.2	276.0 ± 30.1	285.2 ± 28.0
3m	–	–	–	> 10000	199.2 ± 20.0	452.1 ± 36.2
3n	–	–	–	60.2 ± 4.5	861.0 ± 62.0	> 1000
3o	–	–	–	158.1 ± 13.2	819.5 ± 64.3	> 1000
4a	H	H	H	3.2 ± 0.2	3750.0 ± 245.0	156.0 ± 13.4
4b	SC_2H_5	H	H	1.4 ± 0.1	> 10000	> 1000
4e	H	CH_3	H	3.5 ± 0.3	> 10000	264.7 ± 23.0
4f	H	Cl	H	4.3 ± 0.4	> 10000	399.5 ± 20.0
5a	H	H	H	14.1 ± 1.6	> 10000	> 1000
5b	SC_2H_5	H	H	> 10000	> 10000	> 1000
5e	H	CH_3	H	6.6 ± 0.5	> 10000	> 1000
5f	H	Cl	H	6.3 ± 0.4	> 10000	> 1000
DPCPX				3.9	130	4000
NECA				14.0	20	6.2
Cl-IBMECA				120	2100	11

[a] K_i values represent the mean ± SEM of at least three determinations obtained from an iterative curve-fitting procedure (GraphPad Prism, GraphPad). [b] Displacement of specific [^{3}H]DPCPX binding in membranes obtained from CHO cells stably expressing hA_1 AR. [c] Displacement of specific [^{3}H]NECA binding in membranes obtained from CHO cells stably expressing hA_{2A} AR. [d] Displacement of specific [^{125}I]AB-MECA binding in membranes obtained from CHO cells stably expressing hA_3 AR. [e] Data from reference [24].

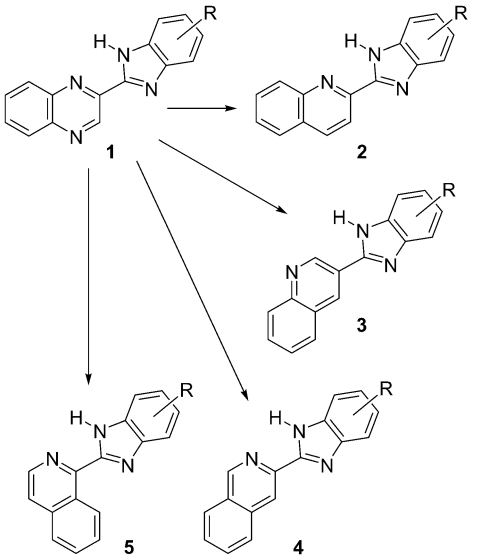

Figure 2. Scaffolds of novel potential AR antagonists **2**–**5** designed as analogues of (1*H*-benzimidazol-2-yl)quinoxalines **1**.

Herein we describe the synthesis and biological and pharmacological evaluation of the following analogues of **1** (Table 1): 2-(1*H*-benzimidazol-2-yl)quinolines (**2a**–**m** and **p**) and their aza isosteres (**2n** and **o**), 3-(1*H*-benzimidazol-2-yl)quinolines (**3a**–**m**) and their aza isosteres (**3n** and **o**), 3-(1*H*-benzimidazol-2-yl)isoquinolines (**4a**, **b**, **e**, and **f**), and 1-(1*H*-benzimidazol-2-yl)isoquinolines (**5a**, **b**, **e**, and **f**).

Results and Discussion

Chemistry

Compounds **2a**–**p** and **3a**–**o** were prepared beginning from quinoline-2-carboxylic acid **6** or quinoline-3-carboxylic acid **7**, respectively, heated in polyphosphoric acid with the appropriate *o*-phenylenediamine (Figure 3). This synthetic procedure (Scheme 1 and 2) was similar to the reported synthesis of **1** beginning from quinoxaline-2-carboxylic acid;[24] however, heating temperatures and workup protocols were optimized to give improved yields (see Experimental Section for details). Series **4** compounds, as well as the compounds in series **5**, were obtained analogously (Scheme 3 and 4 and Experimental), beginning from isoquinoline-3-carboxylic acid **26** and isoquinoline-1-carboxylic acid **27**.

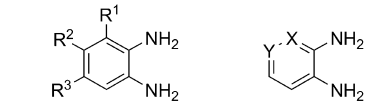

8 $R^1 = R^2 = R^3 = H$
9 $R^1 = SMe$, $R^2 = R^3 = H$
10 $R^1 = Me$, $R^2 = R^3 = H$
11 $R^1 = Cl$, $R^2 = R^3 = H$
12 $R^1 = R^3 = H$, $R^2 = Me$
13 $R^1 = R^3 = H$, $R^2 = Cl$
14 $R^1 = Me$, $R^2 = H$, $R^3 = Cl$
15 $R^1 = R^3 = Cl$, $R^2 = H$
16 $R^1 = H$, $R^2 = R^3 = Me$
17 $R^1 = H$, $R^2 = R^3 = Cl$
18 $R^1 = R^3 = Me$, $R^2 = H$
19 $R^1 = H$, R^2–$R^3 = CH=CH-CH=CH$
20 $R^1 = H$, R^2–$R^3 = CH_2\text{-}CH_2\text{-}CH_2\text{-}CH_2$
21 $R^3 = H$, R^1–$R^2 = CH_2\text{-}CH_2\text{-}CH_2\text{-}CH_2$
22 $R^1 = SEt$, $R^2 = R^3 = H$

23 X = N, Y = CH
24 X = CH, Y = N

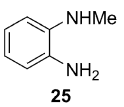

25

Figure 3. Diamines for the syntheses of compounds **2**–**5**.

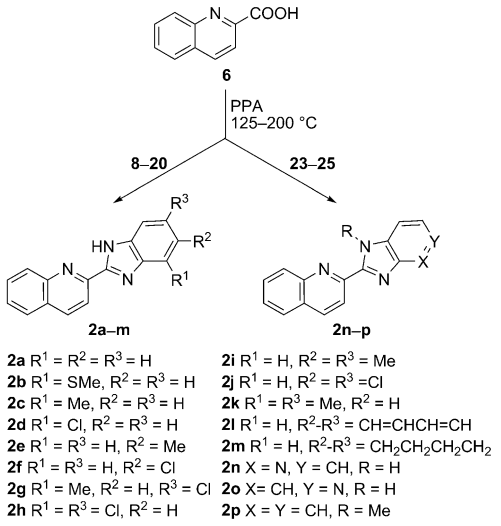

2a $R^1 = R^2 = R^3 = H$
2b $R^1 = SMe$, $R^2 = R^3 = H$
2c $R^1 = Me$, $R^2 = R^3 = H$
2d $R^1 = Cl$, $R^2 = R^3 = H$
2e $R^1 = R^3 = H$, $R^2 = Me$
2f $R^1 = R^3 = H$, $R^2 = Cl$
2g $R^1 = Me$, $R^2 = H$, $R^3 = Cl$
2h $R^1 = R^3 = Cl$, $R^2 = H$
2i $R^1 = H$, $R^2 = R^3 = Me$
2j $R^1 = H$, $R^2 = R^3 = Cl$
2k $R^1 = R^3 = Me$, $R^2 = H$
2l $R^1 = H$, R^2-$R^3 = CH=CHCH=CH$
2m $R^1 = H$, R^2-$R^3 = CH_2CH_2CH_2CH_2$
2n X = N, Y = CH, R = H
2o X= CH, Y = N, R = H
2p X = Y = CH, R = Me

Scheme 1. Synthesis of compounds **2a**–**p**.

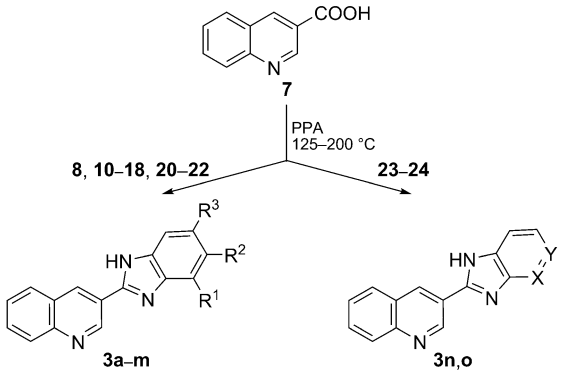

3a $R^1 = R^2 = R^3 = H$
3b $R^1 = SEt$, $R^2 = R^3 = H$
3c $R^1 = Me$, $R^2 = R^3 = H$
3d $R^1 = Cl$, $R^2 = R^3 = H$
3e $R^1 = R^3 = H$, $R^2 = Me$
3f $R^1 = R^3 = H$, $R^2 = Cl$
3g $R^1 = Me$, $R^2 = H$, $R^3 = Cl$
3h $R^1 = R^3 = Cl$, $R^2 = H$
3i $R^1 = H$, $R^2 = R^3 = Me$
3j $R^1 = H$, $R^2 = R^3 = Cl$
3k $R^1 = R^3 = Me$, $R^2 = H$
3l $R^3 = H$, R^1-$R^2 = CH_2\text{-}CH_2\text{-}CH_2\text{-}CH_2$
3m $R^1 = H$, R^2-$R^3 = CH_2\text{-}CH_2\text{-}CH_2\text{-}CH_2$
3n X = N, Y = CH
3o X= CH, Y = N

Scheme 2. Synthesis of compounds **3a**–**o**.

The *o*-phenylenediamines reported in Figure 3 were all commercially available, with the exception of **9**, **20**, **21**, and **22**. Syntheses of **9** and **22** were performed in accordance with our previously reported procedure.[24] Diamines **20** and **21** were obtained beginning from 2-amino-5,6,7,8-tetrahydronaphthalene **28** according to Scheme 5. Briefly, the starting material was initially treated with nitric acid and acetic anhydride to yield nitro derivatives **29** and **30**, which were then separated by flash chromatography (Scheme 5). Deacetylation and reduction furnished compounds **20** and **21** via intermediates **31** and **32**, respectively (Scheme 5).

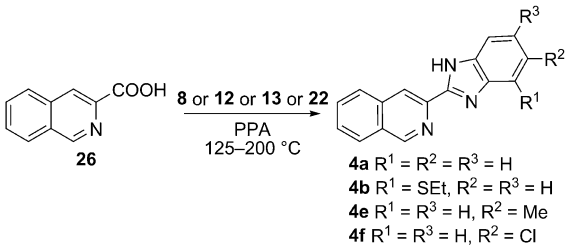

Scheme 3. Synthesis of compounds **4a**, **b**, **e**, and **f**.

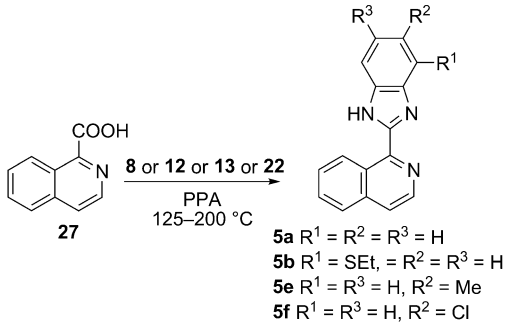

Scheme 4. Synthesis of compounds **5a**, **b**, **e**, and **f**.

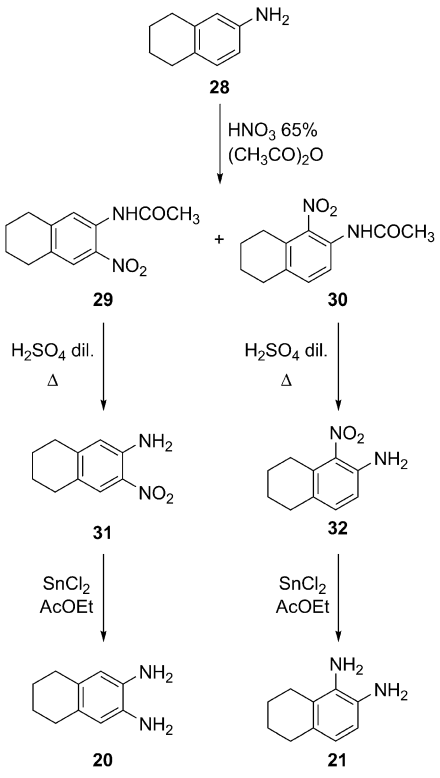

Scheme 5. Synthesis of diamines **20** and **21**.

Biology

Affinities of the new compounds toward human A_1, A_{2A}, and A_3 ARs were evaluated by competition experiments assessing their respective abilities to displace [^{3}H]8-cyclopentyl-1,3-dipropylxanthine ([^{3}H]DPCPX), [^{3}H]adenosine-5′-*N*-ethylcarboxamide ([^{3}H]NECA), or [^{125}I]4-aminobenzyl-5′-*N*-methylcarboxamidoadenosine ([^{125}I]AB-MECA) binding from transfected CHO cells. Experiments were performed as previously described.[26] Compound **4b** and lead **1b** were tested in functional assays against human A_{2B} AR by measuring their effect on NECA-mediated cAMP modulation in transfected CHO cells.

Compound **4b**, which showed high affinity and selectivity for the A_1 AR, was also evaluated for its A_1 AR antagonistic properties on electrically evoked cholinergic contractions in circular smooth muscle preparations of isolated human colon. In these experiments, lead compound **1b** was also tested for purposes of comparison, and the A_1 AR antagonists DPCPX and 8-cyclopentyl-N^3-[3-(4-(fluorosulfonyl)benzoyloxy)propyl]-N^1-propylxanthine (FSCPX) were used as reference compounds. To substantiate the pharmacological results, the expression of A_1 ARs in colonic circular smooth muscle was evaluated by means of reverse transcription–polymerase chain reaction (RT-PCR) analysis.

Discussion

Table 1 lists the binding affinities for the human A_1, A_{2A}, and A_3 ARs of the newly investigated compounds of series **2**–**5** expressed as K_i values. Some of the previously disclosed compounds of series **1**[24] (Figure 4) are also reported in Table 1 for comparison purposes.

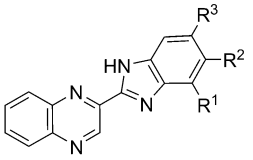

1a $R^1 = R^2 = R^3 = H$
1b $R^1 = SEt$, $R^2 = R^3 = H$
1c $R^1 = SMe$, $R^2 = R^3 = H$
1d $R^1 = Me$, $R^2 = R^3 = H$
1i $R^1 = H$, $R^2 = R^3 = Me$

Figure 4. Benzimidazol-2-yl-quinaxolines **1a**–**d** and **i**.

As a general trend, the molecular scaffolds considered here allow good to moderate binding to the A_1 AR but are unsuitable for binding to the A_{2A} AR and, with a few exceptions, to the A_3 AR as well. Several 2-(1*H*-benzimidazol-2-yl)quinolines **2** exhibit nanomolar potency and good selectivity at the A_1 AR: **2g** (K_i = 2.9 nM), **2f** (K_i = 9.1 nM), **2a** (K_i = 13 nM), **2i** (K_i = 14.5 nM) and **2e** (K_i = 20.7 nM). Compound **2i** stands out for its remarkable selectivity over the A_{2A} and A_3 ARs. With the exception of **2o**, none of the compounds in series **2** binds appreciably to the A_3 AR.

In regards to binding the A_1 AR, the structure–affinity relationships (SARs) of compounds **2** and their isosteres **1**[24] are rather different. Specifically, affinity is maintained by 5,6-dimethyl substitution in series **2** (**2i** versus **2a**) but decreased in series **1** (**1i** versus **1a**). Moreover, a 4-methylthio group is detrimental for potency in series **2** (**2b** versus **2a**) but the same moiety is favorable in series **1** (**1c** versus **1a**). These data suggest that pairs of isosteres belonging to series **1** and **2** do not necessarily adopt similar orientations within the A_1 AR binding site. Elucidation of SARs within series **2** is not a straightforward matter in terms of ligand–A_1 AR interactions. The lack of appreciable affinity for the 4-substituted derivatives **2b**–**d** and the 4,6-disubstituted **2h** and **k** would suggest that the 4- and 6-positions of the benzimidazole ring orient toward sterically forbidden regions within the receptor binding site. However, this hypothesis is not consistent with the excellent affinity of **2g**

($K_i = 2.9$ nM), which has methyl and chlorine moieties at the 4- and 6-positions, respectively. The higher potencies of 5-chloro derivative **2f** ($K_i = 9.1$ nM) and 6-chloro-4-methyl derivative **2g** ($K_i = 2.9$ nM), as compared with their unsubstituted counterpart **2a** ($K_i = 13$ nM), indicate that these small and lipophilic groups insert into hydrophobic pockets of the receptor cavity. The improved affinity of the 5-chloro derivative **2f** ($K_i = 9.1$ nM), as compared with 5-methyl derivative **2e** ($K_i = 20.7$ nM), may be ascribed to the different electron-withdrawing effects of these two substituents. However, this hypothesis is somewhat contradicted by the drastic drop in affinity from 4,5-dimethyl derivative **2i** ($K_i = 14.5$ nM) to 4,5-dichloro derivative **2j** ($K_i > 10000$ nM).

A single substituent at the 4-position is unfavorable for affinity (**2b–d** versus **2a**). Nevertheless, when a chlorine is added to the 6-position of 4-methyl derivative **2c**, yielding **2g**, affinity increases dramatically. A chlorine at the 5-position also results in good affinity (**2f** versus **2a**) but, surprisingly, if a second chlorine is added to the 6-position of 5-chloro derivative **2f** to yield **2j**, affinity is lost. Thus, these data did not allow us to make conclusions about the effect of a 6-chlorine substituent on A_1 AR affinity in series **2**. It is likely that the puzzling SARs outlined above depend on the different conformations and tautomers accessible by our molecules thanks to the freely rotating bond connecting the two heterocyclic systems and the "mobile" benzimidazole NH hydrogen. Encouraged by the high potency of 5,6-dimethyl derivative **2i**, we designed compounds **2l** and **m**, which have a 5,6-fused benzene or cyclohexane ring capable of exploiting hydrophobic interactions with the A_1 AR. Unfortunately, both compounds are devoid of affinity for this receptor, likely due to unfavorable steric factors.

Attempts to improve affinity to any of the ARs by introducing a nitrogen atom as a hydrogen bond acceptor within the benzimidazole nucleus were made through the synthesis of aza isosteres **2n** and **o**. While **2n** is devoid of any appreciable affinity toward the target receptors, **2o** shows a moderate affinity to the A_3 AR ($K_i = 94$ nM) along with excellent selectivity over the A_1 and A_{2A} ARs ($K_i > 10000$ nM for both receptors). The lack of affinity of **2p** to the A_1 AR clearly indicates that the NH group of quinoline derivatives **2** is engaged in a hydrogen bond within the binding site of this receptor and should be therefore regarded as an element of the pharmacophore.

Although a few of the 3-(1*H*-benzimidazol-2-yl)quinolines (**3a–o**) possess nanomolar potency at the A_1 AR (**3a**, **c**, **d**, and **f**), none of these are reasonably selective over the A_{2A} and A_3 ARs. While a 4-ethylthio group strongly improves A_1 AR potency in series **1** (**1b** versus **1a**), the same substitution in series **3** significantly lowers affinity to the A_1 AR, without adding appreciable affinity to the A_{2A} and A_3 ARs (**3b** versus **3a**). In contrast to observations for series **2**, a methyl or chlorine in series **3** at the 4-position of the benzimidazole ring enhances affinity to the A_1 AR (**3c** or **d** versus **3a**). However, in series **3**, similar to what is observed for series **2**, insertion of a chlorine at the 5-position is slightly favorable for potency at the A_1 AR, while incorporation of a methyl group at this position is detrimental (**3e** or **3f** versus **3a**). The 4,6- and the 5,6-disubstituted derivatives **3g–k** are fully devoid of affinity to the A_1 AR. Among this subset of compounds, the 5,6-dimethyl derivative **3i** is notable for its nanomolar potency at the A_3 AR ($K_i = 19$ nM), although this is combined with limited selectivity over the A_{2A} AR. Compounds featuring a 4,5- or 5,6-fused cyclohexane ring (**3l** and **3m**, respectively) as well as the aza isosteres of **3a** (**3n** and **o**) do not exhibit interesting affinity profiles for the ARs examined.

The limited binding data for compounds belonging to series **4** and **5** suggest that affinity across these series is retained or improved by insertion of a small lipophilic substituent at the 4- or 5-position of the benzimidazole ring, with the one exception of **5b** ($R^1 = SC_2H_5$). Series **4** and **5** exhibit the best results in terms of affinity and selectivity at the A_1 AR with respect to the other series analyzed (series **2** and **3**). Compounds **4a**, **b**, **e**, and **f**, as well as **5a**, **e**, and **f** bind to the A_1 AR with K_i values in the nanomolar range and exhibit moderate to excellent selectivity over the A_{2A} and A_3 ARs. The higher potency of **4a** at the A_1 AR as compared with unsubstituted analogues **1a**, **2a**, **3a**, and **5a** suggests that 3-(1*H*-benzimidazol-2-yl)isoquinoline represents the molecular scaffold among the five investigated here that is most suited for selective binding to the A_1 AR (Figure 2). The highest-affinity compound within this subset is **4b**, which has an ethylthio group at the 4-position of the benzimidazole nucleus, analogous to the structure of **1b**. In contrast, 4-ethylthio derivative **5b** is devoid of any appreciable affinity to the ARs. Compound **4b** is slightly less potent than **1b** at the A_1 AR ($K_i = 1.4$ nM versus $K_i = 0.5$ nM, respectively), but significantly more selective over the A_{2A} AR ($K_i > 10$ μM versus $K_i = 3.4$ μM, respectively) and the A_3 AR ($K_i > 1$ μM versus $K_i = 0.95$ μM, respectively). Compounds **1b** and **4b** were also tested against the A_{2B} AR by evaluating their inhibitory effect on NECA-mediated cAMP accumulation in CHO cells stably expressing this receptor subtype. Compound **4b** is completely inactive at this subtype ($K_i > 10$ μM), whereas **1b** displays nanomolar activity in this assay ($IC_{50} = 9.81 \pm 1.07$ nM) while maintaining good selectivity for the A_1 AR. Incidentally, this product may represent a promising lead compound for future development of potent and selective A_{2B} AR antagonists featuring the (1*H*-benzimidazol-2-yl)quinoxaline scaffold.

The high affinity and selectivity of **4b** toward the A_1 AR led to its selection, along with lead compound **1b**, for evaluation of its effects on electrically evoked cholinergic contractions in circular smooth muscle preparations from human colon. Prior to this functional evaluation, we examined the expression of A_1 AR in the target tissues. RT-PCR analysis confirmed the presence of mRNA coding for the A_1 AR in the neuromuscular compartment of colonic specimens. PCR amplification of cDNA coding for A_1 AR was performed under conditions similar to those described by Christofi et al.[27] Following the first run of amplification, cDNA bands were rarely able to be visualized for the A_1 AR. Therefore, PCR products were subjected to a second run of amplification under the same conditions, and DNA bands of the expected size for the A_1 AR were always able to be detected following electrophoretic separation (Figure 5). The identity of the DNA bands was confirmed by sequencing analysis.

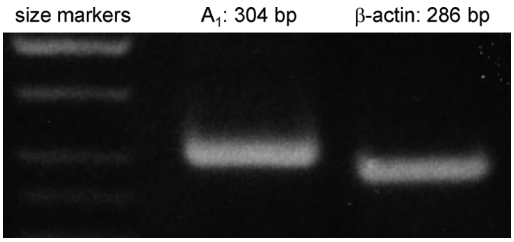

Figure 5. Reverse transcription–polymerase chain reaction (RT-PCR) of A_1 AR and β-actin mRNA in the neuromuscular layer of human distal colon. Representative agarose gel showing the amplification of A_1 AR and β-actin cDNAs.

Functional experiments were then performed to evaluate the effect of **1b** or **4b** on the contractile activity of colonic circular smooth muscle. During the equilibration period, most colonic preparations displayed a rapid spontaneous activity that was low in amplitude and generally stable throughout the experiment. Electrically evoked responses consisted of phasic contractions of variable amplitude, which were abolished by atropine or tetrodotoxin (not shown). Incubation of colonic circular muscle strips with A_1 AR antagonists did not significantly affect spontaneous motor activity.

The incubation of circular muscle strips with A_1 AR antagonists FSCPX (10 nM) or DPCPX (10 nM) induced a significant increase in electrically evoked contractions (+31.4±5.3% and +27.6±4.9%, respectively) (Figure 6). Treatment of colonic specimens with **1b** or **4b** (0.01–10 nM) led to a concentration-dependent increase in electrically evoked cholinergic contractions, with a maximal increment of +32.5±4.3% and +31.6±6.4%, respectively, obtained at 10 nM (Figure 6). In addition, the effects exerted by **1b** (10 nM), **4b** (10 nM), or DPCPX (10 nM) were not altered by co-incubation with FSCPX (1000 nM), indicating that **1b**, **4b**, or DPCPX were sufficient to ensure specific and maximal blockade of A_1 ARs (Figure 6). These findings suggest that the enhancing effect of **1b** or **4b** on electrically induced motility of human colon is highly specific and depends on selective blockade of the A_1 AR.

To better substantiate this hypothesis, a selected concentration of 10 nM was employed in a subsequent series of experiments, where **1b** and **4b** were tested against CCPA, a selective A_1 AR agonist. In colonic preparations maintained in Krebs solution, containing dipyridamole and adenosine deaminase to minimize interferences by endogenous adenosine, electrically evoked cholinergic contractions were decreased by CCPA in a concentration-dependent fashion (EC_{50} = 18.3±3.2 nM; E_{max}: −34.7±4.3%) (Figure 7). Under these conditions, the inhibitory effect exerted by CCPA was antagonized by **1b** (10 nM) (Figure 7A), **4b** (10 nM) (Figure 7B) or DPCPX (10 nM) (Figure 7C) (K_d = 2.54±0.57 nM, 1.08±0.33 nM, and 2.94±0.41 nM, respectively).

Conclusions

We prepared a number of quinolines and isoquinolines connected in various ways to a substituted 1*H*-benzimidazol-2-yl system as potential novel AR antagonists. As a result, we identified **4b** as the ligand exhibiting the best combination of potency at the A_1 AR (K_i = 1.4 nM) and selectivity over A_{2A}, A_{2B}, and A_3 ARs (K_i > 10 μM for A_{2A} and A_{2B}, K_i > 1 μM for A_3). Functional experiments carried out in human circular smooth muscle preparations showed that in vitro application of **4b** or

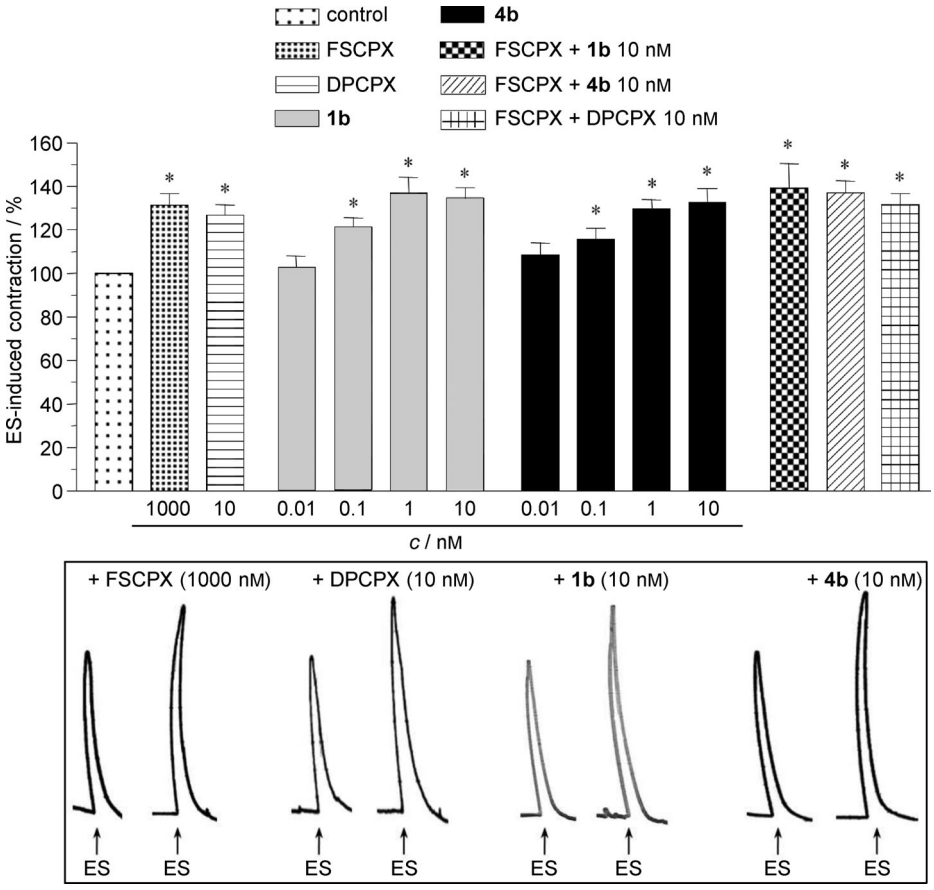

Figure 6. In vitro effects of FSCPX (1000 nM), DPCPX (10 nM), **1b** (0.01–10 nM), **4b** (0.01–10 nM), FSCPX (1000 nM) + **1b** (10 nM), FSCPX (1000 nM) + **4b** (10 nM), or FSCPX (1000 nM) + DPCPX (10 nM) on the contractile responses elicited by electrical stimulations (ES; 10 Hz, 0.5 ms, 30 mA applied as single 10 s train) of circular smooth muscle prepared from human colon maintained in Krebs solution containing guanethidine, NK receptor antagonists, and NPA. Each column represents the mean ±SEM obtained from eight experiments; *p < 0.05: significant difference versus control.

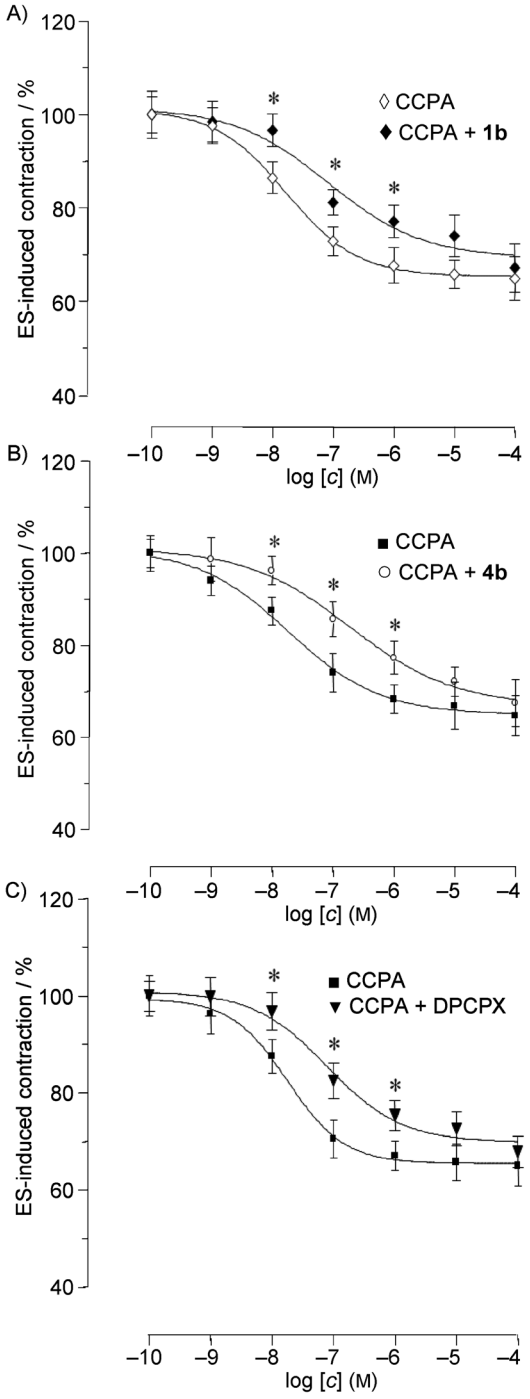

Figure 7. Effects of increasing concentrations of CCPA (0.1–100 μM), alone or in combination with A) **1b** (10 nM), B) **4b** (10 nM), or C) DPCPX (10 nM) on contractions evoked by electrical stimulation (ES; 10 Hz, 0.5 ms, 30 mA applied as repeated 10 s trains every 5 min) of circular smooth muscle prepared from human colon and maintained in Krebs solution containing dipyridamole, adenosine deaminase, guanethidine, NK receptor antagonists, and NPA. Each point represents the mean ± SEM of eight experiments; $*p < 0.05$: significant difference versus CCPA alone.

lead compound **1b**, resulted in a concentration-dependent enhancement of the evoked contractions. The maximal effect of these compounds occurred at 10 nM and was equivalent to that recorded for FSCPX and DPCPX, both known to exert maximal enhancement activity in the same in vitro model at concentrations of 1000 and 10 nM, respectively.[14,28] Notably, neither **1b** nor **4b** affected the motor activity of colonic preparations under resting conditions, and they did not lead to a further increase in the stimulant effect of FSCPX on evoked contractions, suggesting that the enhancing effect of **1b** or **4b** on the electrically induced motility of human colon is highly specific and depends on the selective blockade of A_1 ARs. Moreover, **1b** and **4b**, at the selected concentration of 10 nM, were tested in a subsequent series of experiments against CCPA, a selective A_1 AR agonist. In this setting, CCPA decreased the electrically induced contractions of colonic smooth muscle in a concentration-dependent fashion, and **1b** or **4b** antagonized this inhibitory effect with either a similar or an approximate threefold higher potency than DPCPX, respectively.

In addition, it should be noted that lead compound **1b** (low A_1/A_{2B} AR-selective) and **4b** (fully A_1 AR-selective) presented a similar functional profile, further substantiating the A_1-mediated effects on colonic motility. Overall, the results of these experiments support the evidence that **1b** or **4b** can behave as potent antagonists of A_1 ARs located in the neuromuscular compartment of human colon, and suggest that these compounds may provide a potential starting point for the development of novel agents endowed with stimulant properties on intestinal motility.

Experimental Section

Chemistry

General: Evaporation was performed in vacuo using a rotary evaporator. Analytical TLC was carried out using Merck 0.2 mm precoated silica gel aluminum sheets (60 F_{254}). Silica gel 60 (230–400 mesh) was used for flash column chromatography. Melting points were determined using a Büchi apparatus B 540 and are uncorrected. Routine nuclear magnetic resonance spectra were recorded on a Varian Mercury 400 MHz spectrometer in [D_6]DMSO solution. 1,2-Diamines **9** and **22** were obtained according to a previously reported procedure[24] using 3-chloro-2-nitroaniline as a starting material. Combustion analyses of target compounds were performed by our analytical laboratory in Pisa. All compounds exhibited ≥98% purity.

General procedure 1 for the synthesis of 2a, c, e–g, i, k, 2n, 2o–p, 3a–g, i, j, n, o, and 4b: A mixture of quinoline-2-carboxylic acid **6** (0.50 g, 2.9 mmol), quinoline-3-carboxylic acid **7** (0.50 g, 2.9 mmol), or isoquinoline-3-carboxylic acid **26** (0.50 g, 2.9 mmol), combined with the appropriate diamine (**8**, **10**–**14**, **16**, **18**, **22**–**25**, 2.9 mmol) and polyphosphoric acid (17.5 g) was stirred for 1 h at 125 °C, then for 2 h at 200 °C. The mixture was poured into a large volume of ice water, and the solid mass was collected. The crude product was treated with saturated sodium bicarbonate solution and purified by chromatography to afford the desired derivative. Yields, melting points, and spectral data are reported in the Supporting Information.

General procedure 2 for the synthesis of 2b, d, h, j, l, m, and 3h, k–m: A mixture of quinoline-2-carboxylic acid **6** (0.50 g, 2.9 mmol) or quinoline-3-carboxylic acid 7 (0.50 g, 2.9 mmol), combined with the appropriate diamine (**9**, **11**, **15**, **17**, **19**–**21**, 2.9 mmol) and polyphosphoric acid (17.5 g) was heated for 4 h at

250 °C. After cooling to room temperature, the mixture was poured into a large volume of ice water, and the solid mass was collected by filtration. The crude product was treated with boiling MeOH for 2 h, and charcoal was added. After filtration, the MeOH solution was cooled to precipitate the desired products. Yields, melting points, and spectral data are reported in the Supporting Information.

General procedure 3 for the synthesis of 4a, b, e, f, and 5a, b, e, f: A mixture of isoquinoline-3-carboxylic acid **26** (0.50 g, 2.9 mmol) or isoquinoline-1-carboxylic acid **27** (0.50 g, 2.9 mmol), combined with the appropriate diamine (**8**, **12**, **13**, **22,** 2.9 mmol) and polyphosphoric acid (17.5 g) was stirred for 4 h at 250 °C. After cooling to room temperature, the mixture was poured into a large volume of ice water, and the pH was adjusted to 8.0 with 30% NH_4OH. The solid mass was collected by filtration, washed with water, and dried. Treatment with boiling toluene furnished an extract which, after evaporation, yielded target compounds with the desired degree of purity. Yields, melting points, and spectral data are reported in the Supporting Information.

5,6,7,8-Tetrahydronaphthalene-2,3-diamine 20 and 5,6,7,8-tetrahydronaphthalene-1,2-diamine (21): A solution of 2-amino-3-nitro-5,6,7,8-tetrahydronaphthalene **31** (0.95 g, 4.0 mmol) or 2-amino-1-nitro-5,6,7,8-tetrahydronaphthalene **32** (0.95 g, 4.0 mmol) and tin(II) chloride dihydrate (4.55 g, 20.0 mmol) in EtOAc (65 mL) was stirred at reflux for 2 h. After cooling, the reaction mixture was poured into ice water (200 mL). While stirring, the pH was adjusted to 8.0 with saturated sodium bicarbonate solution, and the resulting precipitate was removed by filtration. The aqueous phase was separated and extracted with EtOAc (4×50 mL). The combined organic phases were dried with Na_2SO_4 and evaporated to dryness to give the desired compounds **20** (88%) or **21** (91%), respectively, which were recrystallized from EtOH.

5,6,7,8-Tetrahydronaphthalene-2,3-diamine (20): mp: 135.3–136.2 °C (lit. [29] 135–136 °C); ^{1}H NMR ([D$_6$]DMSO): δ = 6.18 (s, 2H, H-1 and H-4), 4.15 (br s, 4H, 2×NH_2), 2.48–2.42 (m, 4H, 2×CH_2), 1.65–1.59 ppm (m, 4H, 2×CH_2).

5,6,7,8-Tetrahydronaphthalene-1,2-diamine (21): mp: 85.8–86.7 °C (lit. [29] 84–85 °C); ^{1}H NMR ([D$_6$]DMSO): δ = 6.34 (m, 1H, part A of the system AB), 6.14 (m, 1H, part B of the system AB), 4.16 (br s, 2H, NH_2), 4.05 (br s, 2H, NH_2), 2.53 (pt, 2H, CH_2), 2.36 (pt, 2H, CH_2), 1.75–1.70 (m, 2H, CH_2), 1.69–1.56 ppm (m, 2H, CH_2).

***N*-(3-Nitro-5,6,7,8-tetrahydronaphthalen-2-yl)acetamide (29) and *N*-(1-nitro-5,6,7,8-tetrahydronaphthalen-2-yl)acetamide (30)**: A 1:1 (*v*/*v*) solution of HNO_3 (65%) and acetic anhydride (2.4 mL) was added dropwise to a stirred suspension of 2-amino-5,6,7,8,-tetrahydronaphthalene **28** (13.6 mmol) in acetic anhydride (2.6 mL), maintaining a temperature below 40 °C. Following this addition, the mixture was stirred for 1 h and then treated with ice water (80 mL) to give a yellow precipitate, which was removed by filtration under vacuum, washed with petroleum ether, and dried over NaOH. The crude residue was purified by flash chromatography (petroleum ether/EtOAc, 3:1→2:1 *v*/*v*) to yield compounds **29** and **30** in 36% and 26% yields, respectively. Both **29** and **30** were purified by recrystallization from EtOH.

***N*-(3-Nitro-5,6,7,8-tetrahydronaphthalen-2-yl)acetamide 29**: mp: 134.1–135.0 °C (lit. [30] 133–135 °C); ^{1}H NMR ([D$_6$]DMSO): δ = 10.06 (s, 1H, NH), 7.67 (s, 1H, H-4), 7.33 (s, 1H, H-3), 2.80–2.74 (m, 4H, 2×CH_2), 2.03 (s, 3H, CH_3), 1.76–1.70 ppm (m, 4H, 2×CH_2).

***N*-(1-Nitro-5,6,7,8-tetrahydronaphthalen-2-yl)acetamide 30**: mp: 129.2–129.9 °C (lit. [31] 127 °C); ^{1}H NMR ([D$_6$]DMSO): δ = 9.79 (s, 1H, NH), 7.30–7.21 (m, 2H, system AB), 2.79–2.73 (m, 2H, CH_2), 2.60–2.54 (m, 2H, CH_2), 1.97 (s, 3H, CH_3), 1.75–1.68 ppm (m, 4H, 2×CH_2).

2-Amino-3-nitro-5,6,7,8-tetrahydronaphthalene 31 and 2-amino-1-nitro-5,6,7,8-tetrahydronaphthalene 32: A 1:1 (*v*/*v*) solution of H_2SO_4/H_2O (6 mL) was added slowly at room temperature to a stirred suspension of acetamide **29** or **30** in 10 mL of EtOH. Following this addition, the reaction mixture was heated at reflux for 1 h (TLC, petroleum ether/EtOAc, 3:1 *v*/*v*), then cooled to room temperature. The crude product was poured into ice water (120 mL), and the pH was adjusted to 8.0 with 30% NH_4OH. The resulting yellow–orange precipitate was removed by filtration and treated with 10% HCl (20 mL) until boiling. Compounds **31** (90%) and **32** (65%) were obtained as pure solids by filtration, and were purified by recrystallization from EtOH.

2-Amino-3-nitro-5,6,7,8-tetrahydronaphthalene 31: mp: 124.8–125.6 °C (lit. [29] 124.5–126 °C); ^{1}H NMR ([D$_6$]DMSO): δ = 7.67 (s, 1H, H-4), 7.11 (br s, 2H, NH_2), 6.69 (s, 1H, H-1), 2.66–2.60 (m, 4H, 2×CH_2), 1.69–1.62 ppm (m, 4H, 2×CH_2).

2-Amino-1-nitro-5,6,7,8-tetrahydronaphthalene 32: mp: 96.3–97.4 °C (lit. [29] 94–96 °C); ^{1}H NMR ([D$_6$]DMSO): δ = 6.98 (m, 1H, part A of the system AB), 6.72 (m, 1H, part B of the system AB), 5.87 (br s, 2H, NH_2), 2.61–2.54 (m, 4H, 2×CH_2), 1.70–1.60 ppm (m, 4H, 2×CH_2).

Biology

Adenosine receptor binding assay

Materials: [^{3}H]DPCPX, [^{3}H]NECA, and [^{125}I]AB-MECA were obtained from DuPont–NEN (Boston, MA, USA). ADA was obtained from Sigma–Aldrich (St. Louis, MO, USA). All other reagents were from standard commercial sources and of the highest commercially available grade. CHO cells stably expressing human A_1, A_{2A}, and A_3 ARs were kindly supplied by Prof. K.-N. Klotz, Wurzburg University (Germany).[32]

Human A_1 adenosine receptors: Aliquots of membranes (50 μg protein) obtained from A_1 CHO cells were incubated at 25 °C for 180 min in 500 μL T_1 buffer (50 mM Tris-HCl, 2 mM $MgCl_2$, 2 U mL^{-1} ADA, pH 7.4) containing [^{3}H]DPCPX (3 nM) and six different concentrations of the newly synthesized compounds. Nonspecific binding was determined in the presence of 50 μM RPIA.[26] The dissociation constant (K_d) for [^{3}H]DPCPX in A_1 CHO cell membranes was 3 nM.

Human A_{2A} adenosine receptors: Aliquots of cell membranes (80 μg protein) were incubated at 25 °C for 90 min in 500 μL T_2 buffer (50 mM Tris-HCl, 2 mM $MgCl_2$, 2 U mL^{-1} ADA, pH 7.4) in the presence of 30 nM of [^{3}H]NECA and six different concentrations of the newly synthesized compounds. Nonspecific binding was determined in the presence of 100 μM NECA.[26] The dissociation constant (K_d) for [^{3}H]NECA in A_{2A} CHO cell membranes was 30 nM.

Human A_3 adenosine receptors: Aliquots of cell membranes (40 μg protein) were incubated at 25 °C for 90 min in 100 μL T_3 buffer (50 mM Tris-HCl, 10 mM $MgCl_2$, 1 mM EDTA, 2 U mL^{-1} ADA, pH 7.4) in the presence of 1.4 nM [^{125}I]ABMECA and six different concentrations of the newly synthesized compounds. Nonspecific binding was determined in the presence of 50 μM R-PIA.[26] The dissociation constant (K_d) for [^{125}I]AB-MECA in A_3 CHO cell membranes was 1.4 nM.

All compounds were dissolved in DMSO and diluted with assay buffer to the final concentration, the amount of DMSO never exceeding 2%. Percentage inhibition values for specific radiolabeled

ligand binding at 1–10 μM concentration represent the mean ± SEM of at least three experiments. For compound IC_{50} determination, at least six different ligand concentrations were used. IC_{50} values, which were computer-generated using a nonlinear regression formula (GraphPad Prism, version 3.0 from GraphPad Software Inc., San Diego, CA, USA), were converted into K_i values based on the K_d values of radioligands in the various tissues and using the Cheng and Prusoff equation.[33] K_i values represent the mean ± SEM of at least three determinations.

Measurement of cyclic AMP levels on hA_{2B} CHO cells: Intracellular cyclic AMP (cAMP) levels were measured using a competitive protein binding method.[34] CHO cells expressing recombinant hA_{2B} ARs were harvested by trypsinization. Following centrifugation and resuspension in medium, cells (~48000) were plated in 24-well plates in 0.5 mL medium. After 48 h, the medium was removed, and the cells were incubated at 37 °C for 15 min with 0.5 mL of DMEM in the presence of adenosine deaminase (1 U mL^{-1}) and the phosphodiesterase inhibitor Ro-20-1724 (20 μM). Antagonism profiles for the new compounds toward A_{2B} AR were evaluated by assessing their ability to inhibit 100 nM NECA-mediated accumulation of cAMP. Cells were incubated in the reaction medium for 15 min at 37 °C with various concentrations of the target compound (1 nM–10 μM) and then were treated with NECA. The reaction was terminated by removal of the medium and the addition of 0.4 N HCl. After 30 min, lysates were neutralized with 4 N KOH, and the suspension was centrifuged at 800 g for 5 min. For determination of cAMP production, bovine adrenal cAMP binding protein was incubated with [^{3}H]cAMP (2 nM) and 50 μL cell lysate or cAMP standard (0–16 pmol) at 0 °C for 150 min in a total volume of 300 μL. Protein bound to radioactive compounds was separated by rapid filtration through GF/C glass fiber filters and washed twice with 4 mL 50 mM Tris-HCl, pH 7.4. The radioactivity was measured by liquid scintillation spectrometry.

Pharmacology

Tissue excision and preparation: Specimens of human colon were obtained from patients undergoing surgery for uncomplicated neoplastic conditions. Samples consisted of sections of distal colon from a macroscopically normal region taken at a distance of at least 10 cm from any visible lesion. Care was taken to verify the absence of alterations by histological examination. Portions of tissue were immediately flash frozen in liquid nitrogen and stored at −80 °C for subsequent RT-PCR, or fixed in cold 4% paraformaldehyde, diluted in phosphate buffered saline, for routine histology. The remaining tissue portions were placed into pre-oxygenated Krebs solution and transported on ice to the laboratory, where circular muscle strips ~3 mm in width and 20 mm in length were prepared.[14]

RT-PCR: Colonic tissues were subjected to mucosa and submucosa removal by sharp dissection. Total RNA was isolated from neuromuscular layers by Trizol (Life Technologies, Carlsbad, CA, USA) and chloroform. RNA (1 μg) served as a template for single strand cDNA synthesis by RT in a reaction using 2 μL random hexamers (0.5 μg μL^{-1}) with 200 U Moloney murine leukemia virus (MMLV) reverse transcriptase in manufacturer's buffer containing 500 μM deoxynucleotide triphosphate mixture (dNTP) and 10 mM dithiothreitol (DTT). PCR was performed using primers based on the nucleotide sequence of the cloned human A_1 AR gene.[27] PCR, consisting of 2 μL RT reaction, Taq polymerase 2.5 U, dNTP 100 μM and primers 0.5 μM in a final volume of 50 μL was performed using a T-gradient thermocycler (Biometra, Göttingen, Germany). After 1 min initial denaturation at 94 °C, PCR was performed by 35 cycles of: denaturation at 94 °C (1 min), annealing at 53 °C (30 s), extension at 72 °C (1 min), and final extension at 72 °C (7 min). If no band was detected, PCR was repeated using 2 μL of the initial amplification product with fresh PCR reagents, as previously reported by Christofi et al.[27] Untranscribed RNA was included in PCR reactions to verify the absence of genomic DNA. RT-PCR efficiency was evaluated by primers for human β-actin. Amplified products were separated by 1.5% agarose gel electrophoresis and stained with ethidium bromide. cDNA bands were visualized by UV light.

Recording of circular smooth muscle contractile activity: The contractile activity of human colonic circular smooth muscle was recorded as previously described by Fornai et al.[14] Preparations were set up in organ baths containing Krebs solution (113 mM NaCl, 4.7 mM KCl, 2.5 mM $CaCl_2$, 1.2 mM KH_2PO_4, 1.2 mM $MgSO_4$, 25 mM $NaHCO_3$, and 11.5 mM glucose, pH 7.4 ± 0.1) with guanethidine (adrenergic blocker, 10 μM), N^{ω}-propyl-L-arginine [NPA, selective inhibitor of neuronal nitric oxide (NO) synthase, nNOS; 100 nM], L-732138 (NK_1 receptor antagonist, 10 μM), GR-159897 (NK_2 receptor antagonist, 1 μM) and SB-218795 (NK_3 receptor antagonist, 1 μM) to prevent noncholinergic responses. The solution was maintained at 37 °C and bubbled with 95% O_2 and 5% CO_2. Circular colonic strips were connected to isotonic transducers (Basile, Comerio, Italy) under a constant 1 g load and were allowed to equilibrate for at least 30 min. Colonic muscle activity was recorded by polygraphs (Basile). Field electrical stimulation was delivered by a BM-ST6 stimulator (Biomedica Mangoni, Pisa, Italy). Electrical stimuli (10 Hz, 0.5 ms, 30 mA) were applied as single or repeated 10 s trains. In the latter setting, trains were applied every 5 min. Each preparation was challenged with electrical stimulations, and experiments started when reproducible responses were obtained (usually after 2–3 stimulations).

Design of experiments: In the first set of experiments, the effects of **1b** or **4b** (0.01–10 nM) were evaluated with electrically evoked cholinergic contractions. To verify that **1b**- or **4b**-induced effects resulted specifically from A_1 AR blockade, the selective and irreversible A_1 AR antagonist FSCPX (1000 nM),[28] as well as the selective and reversible antagonist DPCPX (10 nM),[14] were used for comparison. In the second set of experiments, effects of the A_1 AR agonist CCPA (0.1–10000 nM) were tested on electrically evoked cholinergic contractions in the absence and presence of (10 nM) **1b**, **4b**, or DPCPX. Krebs solution was added, along with dipyridamole (adenosine reuptake inhibitor, 500 nM) and adenosine deaminase (enzyme responsible for conversion of adenosine into inosine, 0.5 U mL^{-1}) to abate the extracellular levels of endogenous adenosine.[20]

The effects of compounds tested were expressed as the percentage of changes versus control contractions elicited by electrical stimulation. The apparent potency of CCPA was expressed as EC_{50} (concentration of agonist producing 50% of maximal response). The percentage of maximum inhibition of control motor responses (E_{max}) was also estimated. Both parameters were calculated from concentration–response curves, and the values were averaged. The affinities of **1b**, **4b**, and DPCPX were expressed as K_d values from Equation (1), where B is the molar concentration of the antagonist and DR is the ratio of equally effective concentrations of the agonist (EC_{50}) in the presence and absence of the antagonist.

$$K_d = [B]/(DR-1) \quad (1)$$

Drugs and reagents: Atropine sulfate, guanethidine monosulfate, 8-cyclopentyl-N^3-[3-(4-(fluorosulfonyl)benzoyloxy)propyl]-N^1-propylxanthine (FSCPX, Sigma–Aldrich); tetrodotoxin, L-732138, GR-

159897, SB-218795, N^{ω}-propyl-L-arginine, 8-cyclopentyl-1,3-dipropylxanthine (DPCPX), 2-chloro-N^6-cyclopentyladenosine (Tocris, Bristol, UK). Adenosine receptor ligands were dissolved in DMSO, with further dilutions made using saline solution. DMSO concentration in organ baths was never higher than 0.5%.

Statistical analysis: Results are given as the mean ± SEM. Significant differences were evaluated with raw data prior to percentage normalization using Student's *t* test for paired data or analysis of variance (ANOVA), followed by post hoc analysis with Dunnett's test or Student–Newman–Keul's test, as appropriate; $p < 0.05$ was considered significant. Colonic preparations included in each test group were obtained from different patients; therefore, the number of experiments also refers to the number of patients assigned to each group. EC_{50} values were interpolated from concentration–response curves. Calculations were performed by commercial software (GraphPad Prism, GraphPad Software Inc.).

Acknowledgements

This work was supported financially by MIUR (PRIN-2007) and by the Universities of Napoli and Pisa (Italy). We thank Prof. Dr. Karl-Norbert Klotz for his generous gift of transfected CHO cells expressing human A_1, A_{2A}, A_{2B}, and A_3 adenosine receptors.

Keywords: 1*H*-benzimidazol-2-ylquinolines · adenosine receptors · antagonists · colon motility · lead optimization

[1] S.-A. Poulsen, R. J. Quinn, *Bioorg. Med. Chem.* **1998**, *6*, 619–641.
[2] B. B. Fredholm, G. Arslan, L. Halldner, B. Kull, G. Schulte, W. Wasserman, *Naunyn Schmiedeberg's Arch. Pharmacol.* **2000**, *362*, 364–374.
[3] B. B. Fredholm, A. P. IJzerman, K. A. Jacobson, K.-N. Klotz, J. Linden, *Pharmacol. Rev.* **2001**, *53*, 527–552.
[4] B. B. Fredholm, *Cell Death Differ.* **2007**, *14*, 1315–1323.
[5] G. Schulte, B. B. Fredholm, *Cell. Signalling* **2003**, *15*, 813–827.
[6] K. A. Jacobson, Z. G. Gao, *Nat. Rev. Drug Discov.* **2006**, *5*, 247–264.
[7] S. Moro, Z.-G. Gao, K. A. Jacobson, G. Spalluto, *Med. Res. Rev.* **2006**, *26*, 131–159.
[8] A. K. Dhalla, J. C. Shryock, R. Shreeniwas, L. Belardinelli, *Curr. Top. Med. Chem.* **2003**, *3*, 369–385.
[9] J. Wardas, *Pol. J. Pharmacol.* **2002**, *54*, 313–326.
[10] J. A. Ribeiro, A. M. Sebastião, A. de Mendonça, *Prog. Neurobiol.* **2003**, *68*, 377–392.
[11] R. N. Takahashi, F. A. Pamplona, R. D. Prediper, *Front. Biosci.* **2008**, *13*, 2614–2632.
[12] A. Nishiyama, M. Rahman, E. W. Inscho, *Hypertens. Res.* **2004**, *27*, 791–804.
[13] R. H. Shah, W. H. Frishman, *Cardiol. Rev.* **2009**, *17*, 125–131.
[14] M. Fornai, L. Antonioli, R. Colucci, N. Ghisu, P. Buccianti, A. Marioni, M. Chiarugi, M. Tuccori, C. Blandizzi, M. Del Tacca, *Neurogastroenterol. Motil.* **2009**, *21*, 451–466.
[15] L. Antonioli, M. Fornai, R. Colucci, N. Ghisu, M. Tuccori, M. Del Tacca, C. Blandizzi, *Inflamm. Bowel Dis.* **2008**, *14*, 566–574.
[16] B. Siegmund, F. Rieder, S. Albrich, K. Wolf, C. Bidlingmaier, G. S. Firestein, D. Boyle, H. A. Lehr, F. Loher, G. Hartmann, S. Endres, A. Eigler, *J. Pharmacol. Exp. Ther.* **2001**, *296*, 99–105.
[17] M. Odashima, G. Bamias, J. Rivera-Nieves, J. Linden, C. C. Nast, C. A. Moskaluk, M. Marini, K. Sugawara, K. Kozaiwa, M. Otaka, S. Watanabe, F. Cominelli, *Gastroenterology* **2005**, *129*, 26–33.
[18] L. Antonioli, M. Fornai, R. Colucci, N. Ghisu, F. Da Settimo, G. Natale, O. Kastsiuchenka, E. Duranti, A. Virdis, C. Vassalle, C. La Motta, L. Mugnaini, M. C. Breschi, C. Blandizzi, M. Del Tacca, *J. Pharmacol. Exp. Ther.* **2007**, *322*, 435–442.
[19] M. Kadowaki, Y. Nagakura, K. Tokita, K. Hanaoka, M. Tomoi, *Eur. J. Pharmacol.* **2003**, *458*, 197–200.
[20] L. Antonioli, M. Fornai, R. Colucci, N. Ghisu, C. Blandizzi, M. Del Tacca, *Inflamm. Bowel Dis.* **2006**, *12*, 117–122.
[21] C. La Motta, S. Sartini, L. Mugnaini, S. Salerno, F. Simorini, S. Taliani, A. M. Marini, F. Da Settimo, A. Lavecchia, E. Novellino, L. Antonioli, M. Fornai, C. Blandizzi, M. Del Tacca, *J. Med. Chem.* **2009**, *52*, 1681–1692.
[22] L. Antonioli, M. Fornai, R. Colucci, N. Ghisu, M. Tuccori, M. Del Tacca, C. Blandizzi, *Pharmacol. Ther.* **2008**, *120*, 233–253.
[23] H. Kehlet, K. Holte, *Am. J. Surg.* **2001**, *182*, S3–S10.
[24] E. Novellino, B. Cosimelli, M. Ehlardo, G. Greco, M. Iadanza, A. Lavecchia, M. G. Rimoli, A. Sala, A. Da Settimo, G. Primofiore, F. Da Settimo, S. Taliani, C. La Motta, K.-N. Klotz, D. Tuscano, M. L. Trincavelli, C. Martini, *J. Med. Chem.* **2005**, *48*, 8253–8260.
[25] F. H. Allen, S. Bellard, M. D. Brice, B. A. Cartwright, A. Doubleday, H. Higgs, T. Hummelimk, B. G. Hummelink-Peters, O. Kennard, W. D. S. Motherwell, J. R. Rodgers, D. G. Watson, *Acta Crystallogr.* **1979**, *B35*, 2231–2239.
[26] F. Da Settimo, G. Primofiore, S. Taliani, C. La Motta, E. Novellino, G. Greco, A. Lavecchia, B. Cosimelli, M. Iadanza, K.-N. Klotz, D. Tuscano, M. L. Trincavelli, C. Martini, *Drug Dev. Res.* **2004**, *63*, 1–7.
[27] F. L. Christofi, H. Zhang, J. G. Yu, J. Guzman, J. Xue, M. Kim, Y. Z. Wang, H. J. Cooke, *J. Comp. Neurol.* **2001**, *439*, 46–64.
[28] J. E. Wunderlich, B. J. Needleman, Z. Chen, J. G. Yu, Y. Wang, I. Grants, D. J. Mikami, W. S. Melvin, H. J. Cooke, F. L. Christofi, *Am. J. Physiol. Gastrointest. Liver Physiol.* **2008**, *294*, G554–G566.
[29] G. Schroeter, E. Kindermann, C. Dietrich, C. Beyschlag, Cl. Fleischhauer, E. Riebensahm, C. Oesterlin, *Justus Liebigs Ann. Chem.* **1922**, *426*, 17–83.
[30] E. R. Ward, M. T. Coulson, *J. Chem. Soc.* **1954**, 4545–4547.
[31] E. R. Ward, B. D. Pearson, *J. Chem. Soc.* **1959**, 3378–3383.
[32] K.-N. Klotz, J. Hessling, J. Hegler, C. Owman, B. Kull, B. B. Fredholm, M. J. Lohse, *Naunyn Schmiedeberg's Arch. Pharmacol.* **1998**, *357*, 1–9.
[33] Y. Cheng, W. H. Prusoff, *Biochem. Pharmacol.* **1973**, *22*, 3099–3108.
[34] C. Nordstedt, B. B. Fredholm, *Anal. Biochem.* **1990**, *189*, 231–234.

Received: June 8, 2011
Revised: June 29, 2011
Published online on July 27, 2011

